THE JOURNAL OF BIOLOGICAL CHEMISTRY VOL. 286, NO. 42, pp. 36258–36267, October 21, 2011

Deletion of Betaine-Homocysteine *S*-Methyltransferase in Mice Perturbs Choline and 1-Carbon Metabolism, Resulting in Fatty Liver and Hepatocellular Carcinomas*[S]

Received for publication, May 26, 2011, and in revised form, August 24, 2011 Published, JBC Papers in Press, August 30, 2011, DOI 10.1074/jbc.M111.265348

Ya-Wen Teng[‡], Mihai G. Mehedint[§], Timothy A. Garrow[¶], and Steven H. Zeisel[‡§1]

From the [‡]Department of Nutrition, School of Public Health, University of North Carolina, Chapel Hill, North Carolina 27599, the [§]Nutrition Research Institute, University of North Carolina at Chapel Hill, Kannapolis, North Carolina 28081, and the [¶]Department of Food Science and Human Nutrition, University of Illinois at Urbana-Champaign, Urbana, Illinois 61801

Betaine-homocysteine *S*-methyltransferase (BHMT) uses betaine to catalyze the conversion of homocysteine (Hcy) to methionine. There are common genetic polymorphisms in the *BHMT* gene in humans that can alter its enzymatic activity. We generated the first *Bhmt*$^{-/-}$ mouse to model the functional effects of mutations that result in reduced BHMT activity. Deletion of *Bhmt* resulted in a 6-fold increase ($p < 0.01$) in hepatic and an 8-fold increase ($p < 0.01$) in plasma total Hcy concentrations. Deletion of *Bhmt* resulted in a 43% reduction in hepatic *S*-adenosylmethionine (AdoMet) ($p < 0.01$) and a 3-fold increase in hepatic *S*-adenosylhomocysteine (AdoHcy) ($p < 0.01$) concentrations, resulting in a 75% reduction in methylation potential (AdoMet:AdoHcy) ($p < 0.01$). *Bhmt*$^{-/-}$ mice accumulated betaine in most tissues, including a 21-fold increase in the liver concentration compared with wild type (WT) ($p < 0.01$). These mice had lower concentrations of choline, phosphocholine, glycerophosphocholine, phosphatidylcholine, and sphingomyelin in several tissues. At 5 weeks of age, *Bhmt*$^{-/-}$ mice had 36% lower total hepatic phospholipid concentrations and a 6-fold increase in hepatic triacyglycerol concentrations compared with WT ($p < 0.01$), which was due to a decrease in the secretion of very low density lipoproteins. At 1 year of age, 64% of *Bhmt*$^{-/-}$ mice had visible hepatic tumors. Histopathological analysis revealed that *Bhmt*$^{-/-}$ mice developed hepatocellular carcinoma or carcinoma precursors. These results indicate that BHMT has an important role in Hcy, choline, and one-carbon homeostasis. A lack of *Bhmt* also affects susceptibility to fatty liver and hepatocellular carcinoma. We suggest that functional polymorphisms in *BHMT* that significantly reduce activity may have similar effects in humans.

Betaine-homocysteine *S*-methyltransferase (BHMT)[2] is a zinc-dependent cytosolic enzyme that catalyzes the transfer of a methyl group from betaine to homocysteine (Hcy) forming dimethylglycine and methionine (Met) (Fig. 5). Humans have common single nucleotide polymorphisms in the *BHMT* gene that alter BHMT enzyme activity and function (1). A common *BHMT* single nucleotide polymorphism rs3733890 (41% of NC population has 1 variant allele, and 8% have 2 alleles (2)) was associated with increased risk for having babies with neural tube defects (3), decreased risk for developing cardiovascular disease (4), and reduced risk for breast cancer-specific mortality (5). The epidemiological evidence suggests the importance of single nucleotide polymorphisms in the gene. However, the metabolic consequences of having null mutations of the *BHMT* gene have not been thoroughly investigated. To directly investigate the role of BHMT *in vivo*, we generated and characterized mice in which the gene encoding *Bhmt* was deleted (*Bhmt*$^{-/-}$).

BHMT activity is found at high levels in the liver and kidney, and low levels in the brain, lenses, and other human tissues. In rodents, high levels of BHMT activity are only found in the liver (6). Betaine, the methyl donor for BHMT, comes from either dietary sources or from oxidation of choline (an irreversible reaction) by choline dehydrogenase (CHDH). Alternatively, choline can be used to form the phospholipid phosphatidylcholine (PtdCho) or the neurotransmitter acetylcholine (7). The product of BHMT, methionine, is the precursor for *S*-adenosylmethionine (AdoMet), the major methyl donor for most biological methylations, including DNA and histone methylation, the conversion of glycine to methylglycine (catalyzed by glycine methyltransferase (GNMT)), and the methylation of phosphatidylethanolamine (PtdEtn) to form PtdCho (catalyzed by phosphatidylethanolamine *N*-methyltransferase (PEMT)).

The other substrate for BHMT is Hcy, a thiol-containing amino acid, which, when elevated in plasma, is associated with cardiovascular diseases, pregnancy complications, renal insufficiency, and cognitive impairment (8). Hcy is converted to methionine by BHMT or by methionine synthase, the latter of which uses methyltetrahydrofolate (methyl-THF) as the methyl

* This work was supported, in whole or in part, by National Institutes of Health Grants DK55865 and DK36530 (to S. H. Z.) and DK52501 (to T. A. G.).

[S] The on-line version of this article (available at http://www.jbc.org) contains supplemental Tables S1 and S2.

[1] To whom correspondence should be addressed: 500 Laureate Way, Kannapolis, NC 28081. Tel.: 704-250-5003; Fax: 704-250-5001; E-mail: steven_zeisel@unc.edu.

[2] The abbreviations used are: BHMT, betaine-homocysteine *S*-methyltransferase; MS, methionine synthase; CBS, cystathionine-β-synthase; CγL, cystathionine-γ-lyase; PEMT, phosphatidylethanolamine methyltransferase; GNMT, glycine methyltransferase; CHDH, choline dehydrogenase; Hcy, homocysteine; AdoMet, *S*-adenosylmethionine; AdoHcy, *S*-adenosylhomocysteine; PtdCho, phosphatidylcholine; PtdEth, phosphatidylethanolamine; PCho, phosphocholine; GPCho, glycerophosphocholine; PtdIns, phosphatidylinositol; PtdSer, phosphatidylserine; BUN, plasma urea nitrogen; THF, tetrahydrofolate; NEFA, nonesterified fatty acid; TAG, triacylglycerol; LDH, lactate dehydrogenase; ALT, alanine transaminase; CK, creatinine kinase; HDL-C, high density lipoprotein cholesterol; VLDL, very low density lipoprotein; γGT1, γ-glutamyltransferase 1; HCC, hepatocellular carcinoma.

donor (supplied by methylenetetrahydrofolate reductase) (9). Alternatively, Hcy is removed by the trans-sulfuration pathway, forming cystathionine and cysteine catalyzed by the enzymes cystathionine-β-synthase (CBS) and cystathionine-γ-lyase (CγL), respectively (9). Both enzymes require vitamin B_6; CBS also requires AdoMet as the allosteric activator (9). All the above pathways might be perturbed with the deletion of *Bhmt.* Here, we report on the metabolic phenotype of the first *Bhmt* knock-out mouse created.

EXPERIMENTAL PROCEDURES

Generation of Bhmt$^{-/-}$ Mice—The gene targeting vector was designed to remove exons 6 and 7, the zinc-binding domains of the gene (Fig. 1*A*). The targeting vector was constructed by placing a MC1-neomycin (Neo) selectable marker flanked by 2 flippase (FLP) recognition target (FRT) sites and 1 locus of X-over P1 (loxP) site ~330 bp downstream of exon 7. A second loxP site was introduced ~240 bp upstream of exon 6. The vector was electroporated into E14Tg2A embryonic stem cells. Targeted cells were screened by PCR, confirmed by Southern blot analysis, and injected into blastocysts derived from mouse strain C57Bl/6 to create *Bhmt* transmitting chimeras. Neo deleted mice were generated by crossing the transmitting chimeras with Flpe deleters (number 003800, Jackson Laboratory, Bar Harbor, ME), which expressed Flpe recombinase that recognized FRT sites and deleted the Neo cassette. *Bhmt* knock-out mice were generated by crossing the Neo deleted mice with Cre deleters (number 003724, Jackson Laboratory), which expressed Cre recombinase that recognized loxP sites and deleted exons 6 and 7. *Bhmt* knock-out mice were continuously backcrossed to C57Bl/6 mice. Generations F1 to F4 were used in this study.

For all experiments, *Bhmt*$^{+/+}$, *Bhmt*$^{+/-}$, and *Bhmt*$^{-/-}$ littermates born of *Bhmt*$^{+/-}$ mating pairs were used to control the mixed genetic background. Mice were genotyped by PCR using TaKaRa Ex TaqDNA polymerase (TaKaRa Bio USA, Madison, WI) and the following primer sequences: *Bhmt*$^{+/+}$ forward, 5′-GACTTTTAAAGAGTGGTGGTACATACCTTG-3′, *Bhmt*$^{+/+}$ reverse, 5′-TCTCTCTGCAGCCACATCTGAACTTGTCTG-3′, *Bhmt*$^{-/-}$ forward, 5′-TTAACTCAACATCACAACAACAGATTTCAG-3′, *Bhmt*$^{-/-}$ reverse, 5′-TTGTCGACGGATCCATAACTTCGTATAAT-3′. PCR conditions were as follows: 94 °C for 2 min; 40 cycles of 94 °C for 30 s, 64 °C for 2 min, and 72 °C for 2 min; and 72 °C for 6 min. *Bhmt*$^{+/+}$ PCR product was 1.6 kb in size, whereas *Bhmt*$^{-/-}$ was 545 bp (Fig. 1*B*). The animals were kept in a temperature-controlled environment at 24 °C and exposed to a 12-h light and dark cycle. All animals received AIN-76A pelleted diet with 1.1 g/kg choline chloride (Dyets, Bethlehem, PA). The Institutional Animal Care and Use Committee of the University of North Carolina at Chapel Hill approved all experimental protocols.

Reproducibility, Viability, Body Weight, Body Length, and Life Span—Pairs of *Bhmt*$^{+/+}$, *Bhmt*$^{+/-}$, and *Bhmt*$^{-/-}$ parents were bred to assess their reproductive potential. Sizes, genotype distribution, and gender distribution of litters were recorded. Body weights and lengths (nose to hip, nose to tail) of *Bhmt*$^{+/+}$, *Bhmt*$^{+/-}$, and *Bhmt*$^{-/-}$ mice were measured from age 3.5 to 20 weeks old using a scale and a ruler, respectively. Eleven *Bhmt*$^{+/+}$ and 14 *Bhmt*$^{-/-}$ mice were maintained over the course of a year to determine 1-year survival rates.

Western Blot and Enzymatic Assay—Mice were anesthetized by inhalation of isoflurane (Hospira, Lake Forest, IL). Tissues were harvested, weighted, snap frozen, pulverized under liquid nitrogen, and stored at −80 °C until used. Western blot analysis of BHMT was performed in liver homogenate as previously described (10). For all enzymatic assays, pulverized liver from 5-week-old mice were homogenized in buffer using a motorized tissue homogenizer (Talboys Engineering Corporation, Montrose, PA). BHMT activity was measured as the conversion of [^{14}C]betaine to [^{14}C]methionine and [^{14}C]dimethylglycine as previously described (11). CHDH activity was measured as the conversion of [^{14}C]choline to [^{14}C]betaine as previously described (12) using high pressure liquid chromatography (HPLC) on a Varian ProStar HPLC system (PS-210, Varian Inc., Palo Alto, CA) with a Pecosphere Silica column, 4.6 × 83 mm (PerkinElmer Life Sciences) and a Berthold LB506 C-1 radiodetector (Oak Ridge, TN). GNMT activity was measured as the conversion of [^{3}H]AdoMet to [^{3}H]methylglycine using the charcoal absorption method as previously described (13). PEMT activity was measured as the conversion of [^{3}H]AdoMet to [^{3}H]PtdCho as previously described (14, 15). Protein concentrations were measured using the Bradford Assay (16).

Choline and Homocysteine Metabolites—Tissues from 5-week-old animals were harvested as described above. Blood was collected via cardiac puncture, and plasma was isolated by centrifugation at 3,000 × *g* for 5 min at room temperature. The concentrations of choline metabolites were measured by liquid chromatography-electrospray ionization-isotope dilution mass spectrometry as previously described (17). The concentration of AdoMet and *S*-adenosylhomocysteine (AdoHcy) were measured using the Varian ProStar HPLC system as previously described (18, 19) with an Ultrasphere ODS 5-μm C18 column, 4.6 × 25 cm (number 235329, Fullerton, CA), and a UV-visible detector (model 118, Gilson, Middleton, WI). Plasma total Hcy (tHcy) and cysteine were measured after derivatizing 50 μl of plasma with 7-fluorobenzofurazan-4-sulfonic acid. The derivatized products were measured as previously described (20) using the Varian ProStar HPLC system with a Microsorb-MV 5-μm C18 column, 4.6 mm × 25 cm (Varian) and a Prostar model 360 fluorescence detector (Varian). Mercaptopropinylglycine (10 μM) was used as an internal standard. Hepatic tHcy, cystathionine, methionine, cysteine, methylglycine, dimethylglycine, and glycine were measured as previously described (21) using capillary stable isotope dilution gas chromatography/mass spectrometry (Hewlett-Packard Co., Palo Alto, CA). Plasma total folate was measured using *Lactobacillus casei* assay as previously described (22).

Clinical Analysis—Concentrations of plasma urea nitrogen (BUN) and creatinine as well as activities of lactate dehydrogenase (LDH), alanine transaminase (ALT), and creatinine kinase (CK) were measured using an automatic chemical analyzer (Johnson and Johnson VT250, Rochester, NY) at the Animal Clinical Chemistry and Gene Expression Facility, University of North Carolina, Chapel Hill. Urine-specific gravity was measured using a refractometer (AO Instrument Co., Buffalo, NY) at the Department of Laboratory Animal Medicine Veterinary

and Technical Services Facility, UNC, Chapel Hill. Plasma triacylglycerol (TAG), β-hydroxybutyrate (Stanbio, Boerme, TX), cholesterol, high density lipoprotein cholesterol (HDL-C), nonesterified fatty acids (NEFA), and glucose (Wako, Richmond, VA) were measured colorimetrically per the manufacturer's instructions.

Triacylglycerol, Phospholipids, and Cholesterol—PtdCho, PtdEtn, phosphatidylserine (PtdSer), and phosphatidylinositol (PtdIns) were extracted from the liver of 5-week-old mice using the Bligh and Dyer method (23), and isolated by thin layer chromatography (TLC) (24). Concentrations were determined using a phosphate assay (25). TAG was extracted from liver samples using the Folch method (26) and measured colorimetrically as described above.

In Vivo VLDL Secretion Rate—5-week-old animals were fasted for 4 h. 500 mg/kg body weight of Triton WR1339 (as a 7.5% solution dissolved in PBS) was injected retro-orbitally. Blood samples were taken using heparinized capillary tubes retro-orbitally at 2, 30, 60, and 120 min after Triton WR1339 injection for TAG measurement as an indicator of the secretion rate of the very low density lipoprotein (VLDL).

Tissue Histology—Liver was harvested and fixed in 4% paraformaldehyde, 0.2% gluteraldehyde for 48 h. Liver was processed, paraffin embedded, sectioned at 5 μm, and stained with hemotoxylin and eosin as previously described (27). For tumor analysis, whole liver was sectioned serially, and multiple sections per sample were examined by 2 veterinary pathologists from the Department of Laboratory Animal Medicine, UNC, Chapel Hill. High resolution images were collected using a Zeiss Axiovision A1 upright microscope.

γ-Glutamyltransferase 1 (γGT1)—γGT1 levels were determined using ELISA (Cedarlane, Burlington, NC). Frozen liver samples from 1-year-old mice were homogenized in ice-cold PBS at pH 7.0 containing 10% protease inhibitors (Sigma) using an ultrasonic cell disruptor. The resulting suspension was centrifuged and protein levels were determined by the Lowry method (28). Equal amounts of proteins were loaded onto the ELISA plate according to the manufacturer's protocol. The optical density was read at 450 nm on a Synergy 2 microplate reader (Biotek, VT).

Statistics—Statistical differences were determined using analysis of variance, Tukey-Kramer HSD, and Student's *t* test JMP version 6.0 (SAS Institute, Cary, NC) and reported as mean ± S.E.

RESULTS

Generation and Validation of Bhmt Knock-out Mice—$Bhmt^{-/-}$ mice were generated using a cre/loxP system to delete exons 6 and 7, which contain the zinc-binding domain essential for BHMT activity. The mouse genotype was confirmed by PCR using genomic DNA (Fig. 1*B*). $Bhmt^{-/-}$ mice were also validated by assaying hepatic BHMT activity (Fig. 1*C*) and Western blot (Fig. 1*D*). Deletion of 1 allele of *Bhmt* resulted in a 46% reduction of activity, whereas deletion of both alleles resulted in the absence of activity. BHMT protein is predominantly found in mouse liver and was absent in $Bhmt^{-/-}$ liver.

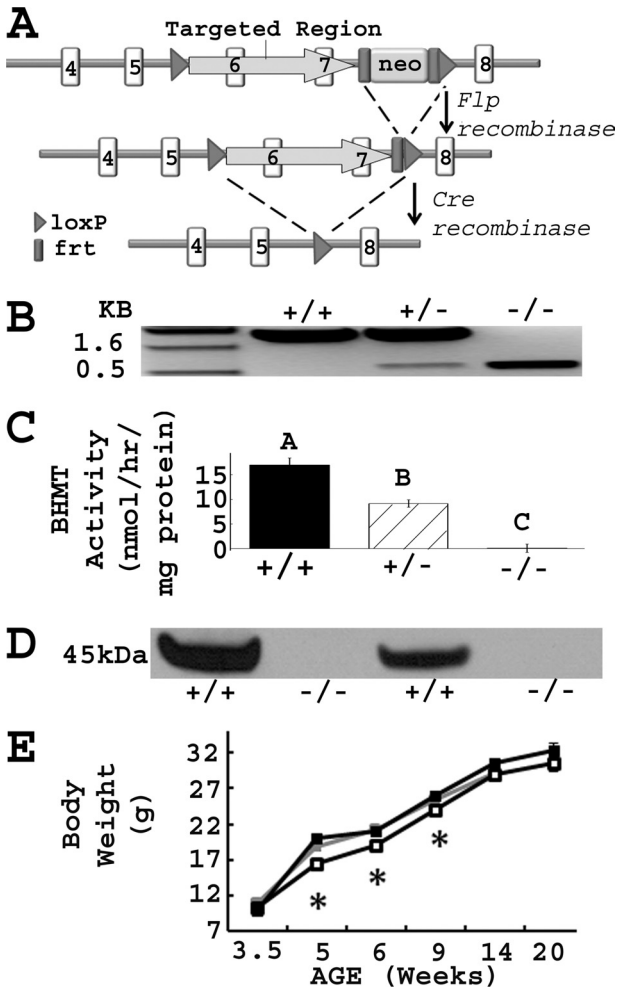

FIGURE 1. **Confirmation of $Bhmt^{-/-}$ mice.** *A*, *Bhmt* chimeric mice were generated using a gene targeting vector that removed exons 6 and 7 of the gene as described under "Experimental Procedures." *loxP*, locus of X-over P1; *frt*, flippase recognition target; *neo*, neomycin cassette; *flp*, flippase recombination enzyme; *cre*, cyclization recombination enzyme. *B*, PCR analysis of genomic DNA isolated from $Bhmt^{+/+}$, $Bhmt^{+/-}$, and $Bhmt^{-/-}$ mice. The PCR product of the WT allele was 1600 bp, whereas the knock-out allele was 545 bp. *C*, hepatic BHMT activity was measured using a radiometric assay in $Bhmt^{+/+}$ (*black bar*), $Bhmt^{+/-}$ (*hatched bar*), and $Bhmt^{-/-}$ (*white bar*) mice. Data are presented as mean ± S.E., $n = 4–8$ per group. Different letters differ significantly ($p < 0.01$) by analysis of variance and Tukey-Kramer HSD tests. *D*, BHMT protein in liver from $Bhmt^{+/+}$ and $Bhmt^{-/-}$ mice were probed by Western blot analysis. The size of the BHMT protein is 45 kDa. *E*, body weights of $Bhmt^{+/+}$ (*black square*), $Bhmt^{+/-}$ (*gray square*), and $Bhmt^{-/-}$ (*white square*) mice were measured using a scale from age 3.5 to 20 weeks old. Data are presented as mean ± S.E., $n = 10–25$ per group. *, $p < 0.05$, different from $Bhmt^{+/+}$ by Student's *t* test.

Bhmt Deletion Had No Effect on Reproductive Capacity or Fetal Viability—Mating pairs of $Bhmt^{+/+}$, $Bhmt^{+/-}$, and $Bhmt^{-/-}$ mice produced offspring with similar litter size (7.5 pups/litter) with evenly distributed genders. $Bhmt^{+/-}$ breeding pairs were used to generate littermates of $Bhmt^{+/+}$, $Bhmt^{+/-}$, and $Bhmt^{-/-}$ mice for all experiments. $Bhmt^{+/-}$ breeding pairs produced offspring at the expected Mendelian ratio, with 24.5% $Bhmt^{+/+}$, 49.7% $Bhmt^{+/-}$, and 25.8% $Bhmt^{-/-}$ mice. The $Bhmt^{+/+}$ and $Bhmt^{-/-}$ mice appeared healthy and lived for at least 1 year.

$Bhmt^{-/-}$ Mice Had Reduced Body Weight at Early Age—Body length and weight of pups were monitored from 3.5 to 20 weeks of age. There was no significant difference in body length

TABLE 1

Deletion of *Bhmt* results in altered choline metabolites in various tissues

Tissues were harvested from 5-week-old $Bhmt^{+/+}$ and $Bhmt^{-/-}$ mice. Choline metabolites were extracted and quantified by liquid chromatography-electrospray ionization-isotope dilution mass spectrometry. Data are presented as mean ± S.E., $n = 5–10$ animals/group.

	Betaine	Choline	GPCho	PCho	PtdCho	Sphingomyelin
Liver						
$Bhmt^{+/+}$	1,321 ± 254	154 ± 36	1,730 ± 554	294 ± 67	15,897 ± 1,200	1,018 ± 131
$Bhmt^{-/-}$	27,314 ± 2,001[a]	28 ± 8[b]	266 ± 38[b]	81 ± 7[b]	11,686 ± 305[b]	838 ± 37
Kidney						
$Bhmt^{+/+}$	1,151 ± 91	779 ± 60	15,608 ± 1,475	853 ± 37	16,088 ± 1,025	3,373 ± 277
$Bhmt^{-/-}$	5,424 ± 505[a]	481 ± 48[b]	10,948 ± 672[c]	792 ± 41	12,707 ± 304[c]	2,685 ± 74[c]
Heart						
$Bhmt^{+/+}$	77 ± 11	84 ± 12	164 ± 7	199 ± 12	11,111 ± 535	879 ± 50
$Bhmt^{-/-}$	1,070 ± 131[a]	49 ± 6[c]	88 ± 10[a]	151 ± 14[c]	8,381 ± 455[b]	583 ± 44[a]
Brain						
$Bhmt^{+/+}$	22 ± 2	183 ± 26	1,208 ± 52	579 ± 33	22,856 ± 1,147	2,191 ± 149
$Bhmt^{-/-}$	100 ± 10[a]	174 ± 15	1,120 ± 57	502 ± 9	21,020 ± 271	1,834 ± 52
Muscle						
$Bhmt^{+/+}$	44 ± 3	67 ± 15	67 ± 4	51 ± 6	7,893 ± 655	411 ± 15
$Bhmt^{-/-}$	529 ± 36[a]	28 ± 3[c]	58 ± 6	18 ± 3[a]	5,942 ± 238[c]	390 ± 13
Adipose						
$Bhmt^{+/+}$	142 ± 25	73 ± 12	802 ± 223	90 ± 6	2,500 ± 217	156 ± 14
$Bhmt^{-/-}$	284 ± 18[a]	34 ± 5[b]	246 ± 79[c]	29 ± 7[c]	2,288 ± 271	144 ± 18
Lung						
$Bhmt^{+/+}$	206 ± 17	198 ± 24	3,586 ± 348	551 ± 26	14,693 ± 344	2,389 ± 65
$Bhmt^{-/-}$	2,237 ± 123[a]	188 ± 23	2,063 ± 82[a]	465 ± 42	14,437 ± 192	2,387 ± 47
Plasma						
$Bhmt^{+/+}$	48 ± 3	20 ± 4	ND[d]	ND	1,590 ± 81	145 ± 10
$Bhmt^{-/-}$	772 ± 173[a]	13 ± 2	ND	ND	1,098 ± 71[a]	114 ± 77
Testis						
$Bhmt^{+/+}$	2,014 ± 312	298 ± 51	809 ± 26	3,831 ± 270	5,760 ± 387	886 ± 74
$Bhmt^{-/-}$	2,018 ± 111	241 ± 10	565 ± 47	3,706 ± 234	5,942 ± 233	954 ± 38

[a] $p < 0.001$ different from $Bhmt^{+/+}$ by Student's *t* test. Concentrations are expressed as nmol/g, except for plasma, which is nmol/ml.
[b] $p < 0.01$, different from $Bhmt^{+/+}$ by Students' *t* test. Concentrations are expressed as nmol/g, except for plasma, which is nmol/ml.
[c] $p < 0.05$, different from $Bhmt^{+/+}$ by Students' *t* test. Concentrations are expressed as nmol/g, except for plasma, which is nmol/ml.
[d] ND, not detected.

among $Bhmt^{+/+}$, $Bhmt^{+/-}$, and $Bhmt^{-/-}$ mice (data not shown), and in body weight between $Bhmt^{+/+}$ and $Bhmt^{+/-}$ mice (Fig. 1*E*). $Bhmt^{-/-}$ mice started with similar body weights as did $Bhmt^{+/+}$ mice at weaning (3.5 weeks), but gained less weight between 5 and 9 weeks of age ($p < 0.05$). The weight difference did not persist after 9 weeks of age.

Bhmt Deletion Resulted in Altered Concentrations of Choline and Its Metabolites—Bhmt is predominantly found in the liver, however, complete deletion of *Bhmt* ($Bhmt^{-/-}$) resulted in a substantial increase in concentrations of betaine in liver (by 21-fold; $p < 0.001$), kidney (by 5-fold; $p < 0.001$), heart (by 14-fold; $p < 0.001$), brain (by 5-fold; $p < 0.001$), muscle (by 12-fold; $p < 0.001$), adipose (by 2-fold; $p < 0.001$), lung (by 11-fold; $p < 0.001$), and plasma (by 16-fold; $p < 0.001$) compared with $Bhmt^{+/+}$ mice (Table 1). Deletion of *Bhmt* resulted in reduced concentrations of choline in liver (by 82%; $p < 0.01$), kidney (by 38%; $p < 0.01$), heart (by 42%; $p < 0.05$), and adipose (by 53%; $p < 0.01$) compared with $Bhmt^{+/+}$ mice. Deletion of *Bhmt* resulted in reduced concentrations of PtdCho in liver (by 26%; $p < 0.01$), kidney (by 21%; $p < 0.05$), heart (by 25%; $p < 0.01$), muscle (by 25%; $p < 0.05$), and plasma (by 31%; $p < 0.001$) compared with $Bhmt^{+/+}$ mice. Deletion of *Bhmt* resulted in reduced concentrations of phosphocholine (PCho) in liver (by 72%; $p < 0.01$), heart (by 24%; $p < 0.05$), muscle (by 65%; $p < 0.001$), and adipose (by 68%; $p < 0.01$) compared with $Bhmt^{+/+}$ mice. Deletion of *Bhmt* resulted in reduced concentrations of glycerophosphocholine (GPCho) in liver ($p < 0.01$), kidney ($p < 0.05$), heart ($p < 0.001$), adipose ($p < 0.05$), and lung ($p < 0.01$), as well as reduced concentrations of sphingomyelin in kidney ($p < 0.05$) and heart ($p < 0.001$) compared with $Bhmt^{+/+}$ mice. In testis, there was no change in any choline metabolites in $Bhmt^{-/-}$ mice. Deletion of 1 copy of *Bhmt* ($Bhmt^{+/-}$) resulted in choline metabolite concentrations in tissues similar to those of $Bhmt^{+/+}$ mice (supplemental Table S1).

Bhmt Deletion Resulted in Altered Concentrations of Hcy, AdoMet, AdoHcy, and Related Metabolites—In liver, complete deletion of *Bhmt* resulted in a 43% decrease in AdoMet concentrations ($p < 0.01$), and a 2.6-fold increase in AdoHcy concentrations ($p < 0.01$), resulting in a 76% reduction in methylation potential (AdoMet:AdoHcy) ratios (0.9 ± 0.1 in $Bhmt^{-/-}$ *versus* 3.6 ± 0.2 in $Bhmt^{+/+}$; $p < 0.01$) (Table 2). $Bhmt^{-/-}$ mice also had reduced hepatic concentrations of dimethylglycine (by 95%; $p < 0.001$), but had increased hepatic concentrations of tHcy (by 6-fold; $p < 0.01$) and methylglycine (by 2.6-fold; $p < 0.05$) compared with $Bhmt^{+/+}$ mice. Hepatic cystathionine, cysteine, methionine, and glycine did not differ among genotypes. In plasma, deletion of *Bhmt* resulted in increased concentrations of tHcy (by 7.8-fold; $p < 0.001$), decreased concentrations of cysteine (by 48%; $p < 0.01$), and decreased concentrations of total folate (by 35%; $p < 0.01$) compared with plasma from $Bhmt^{+/+}$ mice. Deletion of 1 copy of *Bhmt* ($Bhmt^{+/-}$) did not result in changes in hepatic methylation potential, plasma tHcy, or plasma total folate compared with $Bhmt^{+/+}$ mice (supplemental Table S2). $Bhmt^{+/-}$ had plasma cysteine concentrations between those of $Bhmt^{+/+}$ and $Bhmt^{-/-}$ mice.

TABLE 2

Deletion of *Bhmt* results in reduced methylation potential and increased homocysteine concentrations

Tissues were harvested from 5-week-old $Bhmt^{+/+}$ and $Bhmt^{-/-}$ mice. Hepatic homocysteine metabolites were quantified by capillary stable isotope dilution gas chromatography/mass spectrometry. Hepatic AdoMet, AdoHcy, and plasma total homocysteine and cysteine were quantified by high pressure liquid chromatography. Plasma total folate was quantified by a microbial (*L. casei*) assay. Data are presented as mean ± S.E., $n = 5–6$ per group.

Organ	Metabolites	$Bhmt^{+/+}$	$Bhmt^{-/-}$
Liver	AdoMet (nmol/g tissue)	76.4 ± 3.7	43.5 ± 5.7[a]
	AdoHcy (nmol/g tissue)	21.8 ± 1.7	54.4 ± 7.7[a]
	AdoMet:AdoHcy	3.6 ± 0.2	0.9 ± 0.1[a]
	tHomocysteine (nmol/g tissue)	4.2 ± 0.3	26.5 ± 5.5[a]
	Methionine (nmol/g tissue)	223 ± 26	242 ± 23
	Dimethylglycine (nmol/g tissue)	48.2 ± 19.0	2.2 ± 0.2[a]
	Methylglycine (nmol/g tissue)	20.2 ± 8.9	52.7 ± 12.2[b]
	Cystathionine (nmol/g tissue)	32.0 ± 15.7	20.3 ± 5.8
	Cysteine (nmol/g tissue)	247 ± 25	291 ± 25
	Glycine (nmol/g tissue)	1,659 ± 128	1,561 ± 135
Plasma	tHomocysteine (μM)	6.5 ± 0.7	50.8 ± 5.9[a]
	Cysteine (μM)	131.1 ± 9.9	68.4 ± 9.3[a]
	tFolate (ng/ml)	81.7 ± 6.4	52.8 ± 5.1[a]

[a] $p < 0.01$, different from $Bhmt^{+/+}$ by Student's *t* test.
[b] $p < 0.05$, different from $Bhmt^{+/+}$ by Student's *t* test.

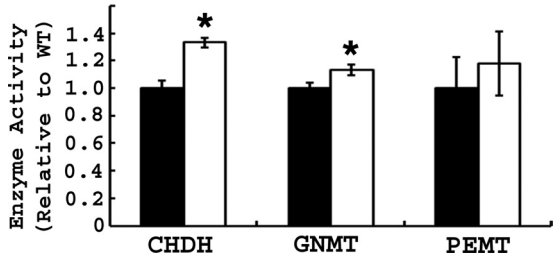

FIGURE 2. ***Bhmt*$^{-/-}$ mice have altered activities of enzymes involved in one-carbon metabolism.** CHDH, GNMT, and PEMT activities were measured in 5-week-old $Bhmt^{+/+}$ (*black bar*) and $Bhmt^{-/-}$ mice (*white bar*) mouse liver using radiometric assays. Data are presented as mean ± S.E., $n = 6–8$ per group. *, $p < 0.05$, different from $Bhmt^{+/+}$ by Student's *t* test.

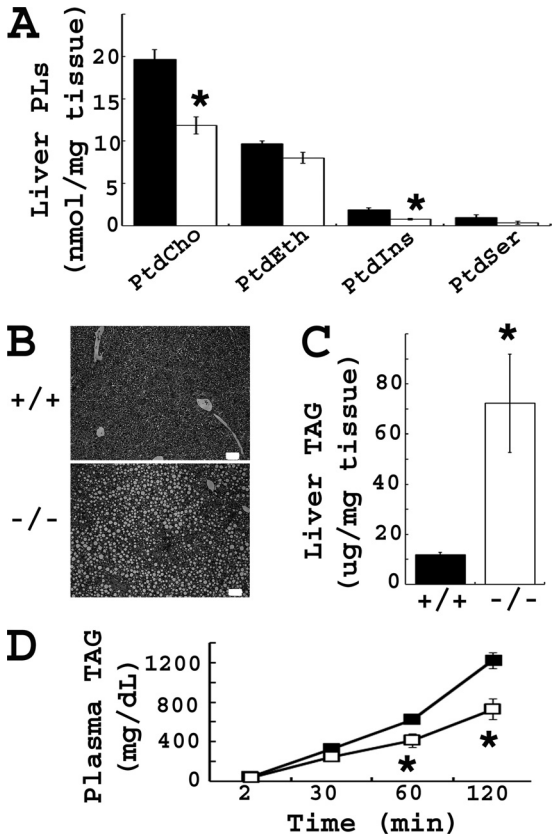

FIGURE 3. ***Bhmt*$^{-/-}$ mice have fatty liver and reduced hepatic phospholipid concentrations.** *A*, hepatic phospholipids of 5-week-old $Bhmt^{+/+}$ (*black bar*) and $Bhmt^{-/-}$ (*white bar*) mice were analyzed by a thin layer chromatography-phosphate assay method. Data are presented as mean ± S.E., $n = 5$ per group. *, $p < 0.01$, different from $Bhmt^{+/+}$ by Student's *t* test. *B*, morphology of liver from 5-week-old mice was shown by H&E staining at ×100 magnification. *Scale bar* = 50 μm. *C*, hepatic TAG of 5-week-old $Bhmt^{+/+}$ (*black bar*) and $Bhmt^{-/-}$ (*white bar*) mice was extracted and quantitated by a colorimetric assay. Data are presented as mean ± S.E., $n = 6–8$ per group. *, $p < 0.05$, different from $Bhmt^{+/+}$ by Student's *t* test. *D*, VLDL secretion rate of 5-week-old $Bhmt^{+/+}$ (*black square*) and $Bhmt^{-/-}$ (*white square*) mice was determined by measuring the plasma TAG after lipoprotein lipase inhibitor injection. Data are presented as mean ± S.E., $n = 6$ per group. *, $p < 0.05$, different from $Bhmt^{+/+}$ by Student's *t* test. *PLs*, phospholipids.

Bhmt Deletion Resulted in Altered Activities of Enzymes Involved in One-carbon Metabolism—Because $Bhmt^{-/-}$ mice (but not $Bhmt^{+/-}$ mice) had altered one-carbon metabolites, enzymes involved in one-carbon metabolism were measured in $Bhmt^{+/+}$ and $Bhmt^{-/-}$ mouse liver. Complete deletion of *Bhmt* resulted in increased hepatic CHDH (by 1.33-fold; $p < 0.05$) and GNMT (by 1.13-fold; $p < 0.05$) activities (Fig. 2). Hepatic PEMT activity was not affected by *Bhmt* deletion.

Bhmt Deletion Resulted in Increased Hepatic Fat Accumulation and Decreased Phospholipids—At 5 weeks of age, hepatic TAG concentrations were 6.5-fold higher in $Bhmt^{-/-}$ mice than in $Bhmt^{+/+}$ mice ($p < 0.05$) (Fig. 3*C*). $Bhmt^{+/-}$ mice had similar hepatic TAG concentrations compared with that of $Bhmt^{+/+}$ mice (8.96 ± 1.92 μg/mg of tissue in $Bhmt^{+/-/-}$ *versus* 11.75 ± 0.99 μg/mg of tissue in $Bhmt^{+/+}$). The difference in hepatic steatosis between $Bhmt^{+/+}$ and $Bhmt^{-/-}$ mice was easily visible at the microscopic level (Fig. 3*B*). Hepatic and plasma phospholipids were measured in $Bhmt^{+/+}$ and $Bhmt^{-/-}$ mouse liver due to their involvement with hepatic lipid storage and release. $Bhmt^{-/-}$ mice had lower concentrations of phospholipids in liver than $Bhmt^{+/+}$ mice (Fig. 3*A*); with a 40% reduction in PtdCho ($p < 0.01$), and a 60% reduction in PtdIns ($p < 0.01$). $Bhmt^{-/-}$ mice also had a 31% reduction in plasma concentrations of PtdCho compared with $Bhmt^{+/+}$ mice ($p < 0.01$) (Table 1). PtdEth concentrations in liver and plasma were the same for both genotypes. $Bhmt^{-/-}$ mice had a significantly reduced VLDL secretion rate (Fig. 3*D*).

Bhmt Deletion Resulted in Altered Clinical Analyses—Plasma alanine aminotransferase activity, a measure of liver damage, was modestly increased in $Bhmt^{-/-}$ mice (34.7 ± 4.4 units/liter in $Bhmt^{-/-}$ *versus* 20.6 ± 4.9 units/liter in $Bhmt^{+/+}$; $p < 0.05$) (Table 3). Plasma BUN, creatinine, CK, and LDH, tests of kidney and muscle function, showed no changes in the $Bhmt^{-/-}$ mice. Urine-specific gravity was significantly reduced in $Bhmt^{-/-}$ mice (1.020 ± 0.002 mg/dL in $Bhmt^{-/-}$ *versus* 1.039 ± 0.005 mg/dL in $Bhmt^{+/+}$; $p < 0.01$). Plasma TAG, glucose, NEFA, and β-hydroxybutyrate concentrations did not differ between genotypes. Compared with wild type littermates, $Bhmt^{-/-}$ mice had significantly lower plasma total cholesterol concentrations (by 45%, $p < 0.01$) and HDL-C (by 38%, $p < 0.01$). Heterozygous mice had similar plasma ALT, BUN, creatinine, LDH, CK, TAG, glucose, NEFA, and β-hydroxybutyrate concentrations compared with wild type mice (supplemental Table S2). Heterozygous mice had no change in plasma

TABLE 3

Deletion of *Bhmt* results in altered metabolic markers

Plasma was collected from 5-week-old $Bhmt^{+/+}$ and $Bhmt^{-/-}$ mice after 4 h fasting. Concentrations of plasma ALT, BUN, creatinine, and activities of LDH and CK were quantitated by the Animal Clinical Chemistry and Gene Expression Facility, UNC, Chapel Hill. Plasma triacylglycerol, cholesterol, HDL cholesterol, glucose, NEFA, hydroxybutyrate were measured colorimetrically. Urine specific gravity was measured by the Department of Laboratory Animal Medicine Veterinary and Technical Services Facility, UNC, Chapel Hill. Data are presented as mean ± S.E., $n = 5–7$ per group.

Organ	Clinical markers	$Bhmt^{+/+}$	$Bhmt^{-/-}$
Plasma	ALT (units/liter)	20.6 ± 4.9	34.7 ± 4.4[a]
	BUN (mg/dL)	12.5 ± 0.8	13.0 ± 1.8
	Creatinine (mg/dL)	<0.1	<0.1
	LDH (units/liter)	841 ± 67	689 ± 80
	CK (units/liter)	741 ± 147	511 ± 147
	Triacylglycerol (mg/dL)	60.9 ± 7.7	47.2 ± 7.9
	Cholesterol (mg/dL)	57.8 ± 4.3	31.6 ± 4.3[b]
	HDL-Cholesterol (mg/dL)	45.8 ± 3.2	26.7 ± 5.7[b]
	Glucose (mg/dL)	292.5 ± 33.2	226.0 ± 15.9
	NEFA (mM)	0.44 ± 0.08	0.28 ± 0.07
	Hydroxybutyrate (mM)	0.39 ± 0.08	0.29 ± 0.03
Urine	Specific gravity (mg/dL)	1.039 ± 0.005	1.020 ± 0.002[b]

[a] $p < 0.05$, different from $Bhmt^{+/+}$ by Student's *t* test.
[b] $p < 0.01$, different from $Bhmt^{+/+}$ by Student's *t* test.

cholesterol and HDL-C concentrations compared with $Bhmt^{+/+}$ mice.

Bhmt Deletion Resulted in Preneoplastic, Neoplastic, and Regenerative Lesions in the Mouse Liver—Eleven $Bhmt^{+/+}$ and 14 $Bhmt^{-/-}$ mice were maintained over the course of a year to determine 1-year survival rates. At time of sacrifice, 64% (9 of 14) of $Bhmt^{-/-}$ mice and 0% (0 of 11) of $Bhmt^{+/+}$ mice had visible hepatic tumors (Fig. 4*A*). Tumors observed in $Bhmt^{-/-}$ mice were solitary or multifocal, found in multiple liver lobes. The average liver weight of $Bhmt^{-/-}$ mice was heavier than that of $Bhmt^{+/+}$ mice (6.22 ± 2.11% BW in $Bhmt^{-/-}$ *versus* 4.36 ± 0.26% BW in $Bhmt^{+/+}$; $p < 0.001$), attributable to tumor mass. A subset of the liver samples (4 of 11 $Bhmt^{+/+}$ livers, 6 of 9 $Bhmt^{-/-}$ livers with tumors, and 4 of 5 $Bhmt^{-/-}$ livers without tumors) were serial-sectioned entirely, stained with H&E, and send to two veterinary pathologists for diagnosis. Microscopic analysis depicted a series of histological abnormalities from preneoplastic lesions (acidophilic/eosinophilic cell foci) to frank neoplasia visible only in the $Bhmt^{-/-}$ mice (Table 4 and

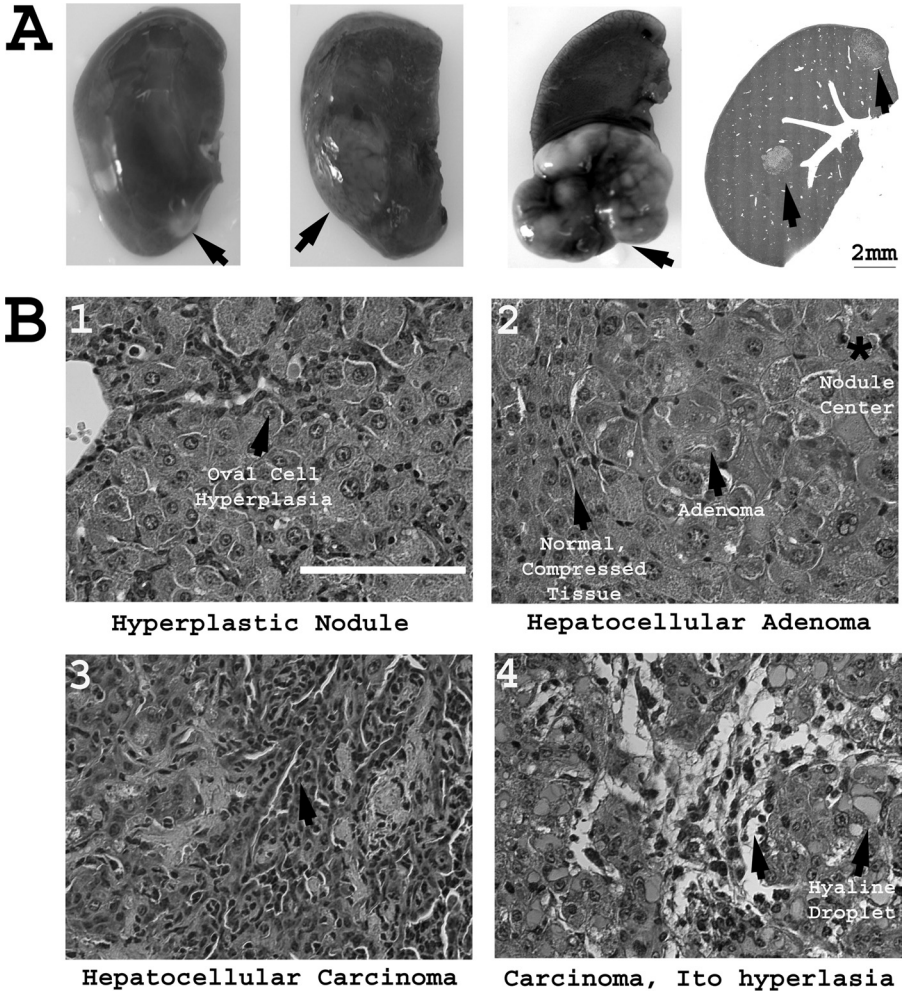

FIGURE 4. ***Bhmt* deletion results in liver tumors at 1 year of age.** *A*, visible hepatic tumors in 1-year-old $Bhmt^{-/-}$ male mice. The inspection of liver specimens at ×4 magnification revealed single or multiple nodules up to 8 mm in diameter. *B*, H&E images of tumor bearing livers at ×400 magnification, showing representative hepatocellular carcinoma and adenoma morphology. *Scale bar*, 50 μm. *1*, regenerative hyperplastic nodule containing streams of proliferative oval and biliary cells; *2*, hepatocellular adenoma (*, center of the nodule) well circumscribed with lobular structure absent, compressive borders, and eosinophilic hepatocytes; *3*, hepatocellular carcinoma represented by a large mass of abnormal vacuolated hepatocytes, containing poorly demarcated areas of smaller hepatocytes with less vacuolization, amphophilic cytoplasm, and a streaming growth pattern (*arrow*); *4*, hepatocellular carcinoma nodule of variably sized hepatocytes exhibiting cytomegaly with hyaline droplets, small hepatocytes with streaming growth pattern, oval cell proliferation, Ito cell proliferation between cords (*unlabeled arrow*), and infiltration of leukocytes.

TABLE 4

Pathology in livers from a subset of 1-year-old *Bhmt*$^{+/+}$ and *Bhmt*$^{-/-}$ mice

A subset of 1-year-old *Bhmt*$^{+/+}$ (4 out of 11, none had visible tumors) and *Bhmt*$^{-/-}$ mouse liver (6 out of 9 that had visible tumors, 4 out of 5 that did not have visible tumors) were serial-sectioned, H&E stained, and send to 2 veterenary pathologists for diagnosis. Dots indicated the changes observed in a particular sample.

Genotype	Visible tumor	HCA	HCC	Fat accumulation	Cellular alteration	Hyperplasia
Bhmt$^{+/+}$				●	●	
Bhmt$^{+/+}$						
Bhmt$^{+/+}$						
Bhmt$^{+/+}$						
Bhmt$^{-/-}$	●	●		●	●	●
Bhmt$^{-/-}$	●	●		●	●	●
Bhmt$^{-/-}$	●	●	●			●
Bhmt$^{-/-}$	●		●		●	
Bhmt$^{-/-}$	●		●	●		●
Bhmt$^{-/-}$	●		●			
Bhmt$^{-/-}$				●	●	●
Bhmt$^{-/-}$					●	
Bhmt$^{-/-}$						●
Bhmt$^{-/-}$					●	

Fig. 4*B*). Hepatocellular adenomas were found in 30% (3 of 10) of the analyzed *Bhmt*$^{-/-}$ livers and none were found in the control animals. These benign lesions were represented by single or multiple nodules, sharply demarcated from the surrounding tissues, with a mild to moderate compression border and loss of lobular structure. Hepatocellular carcinomas (HCC) were found in 50% (5 of 10) of the analyzed *Bhmt*$^{-/-}$ livers. HCC were represented by nodules of atypical, megalohepatocytes that were vacuolated or contained hyaline droplets. Indicative of malignancy, these lesions were organized in cords that were 5–6 cells wide, had poor or nonexisting interface with the surrounding tissues, and compressed mildly the adjacent normal cords. The portal triads and sinusoids were poorly or nondistinguishable in most of the nodules. Formation of heptocellular adenomas and HCC in *Bhmt*$^{-/-}$ mice were accompanied by macro- and microvesicular steatosis, and stellate (Ito) cell and/or oval (bililary) cell hyperplasia (Table 4). We did not study *Bhmt*$^{+/-}$ mouse survival or carcinogenesis.

Bhmt Deletion Resulted in Elevated γ Glutamyltransferase 1 in Livers—γGT1 is a highly sensitive marker of chronic liver disease, neoplasia, and HCC (29). *Bhmt*$^{-/-}$ mice had hepatic γGT1 concentrations 3.3-fold higher than that of the control mice (0.815 ± 0.049 ng/mg of tissue in *Bhmt*$^{-/-}$ *versus* 0.245 ± 0.085 ng/mg of tissue in *Bhmt*$^{+/+}$; $p < 0.01$).

Changes in Choline and One-carbon Metabolites at 5 Weeks Persisted at 1-Year-old Bhmt$^{-/-}$ *Mice*—Choline deficiency and reduced methylation potential have been hypothesized as mechanisms underlying development of HCC. Compared with wild type mice, *Bhmt*$^{-/-}$ mice had a 91% reduction in hepatic methylation potential (AdoMet:AdoHcy) compared with *Bhmt*$^{+/+}$ mice ($p < 0.001$) at 1 year (Table 5), which was greater than the 76% reduction seen at 5 weeks of age (Table 2). The reduced methylation potential was due to reduced hepatic AdoMet (by 50%; $p < 0.01$) and to elevated AdoHcy (by 5.5-fold; $p < 0.001$) concentrations in *Bhmt*$^{-/-}$ mice compared with *Bhmt*$^{+/+}$ mice. Compared with wild type littermates, *Bhmt*$^{-/-}$ mice had a 30-fold increase in hepatic betaine, a 73% reduction in GPCho, a 64% reduction in PCho, and an 18.8% reduction in PtdCho concentrations. At 1 year old, *Bhmt*$^{-/-}$ mice still had an elevated plasma tHcy concentration (by 6.9-fold; $p < 0.01$), but no longer had decreased plasma cysteine concentration.

TABLE 5

Metabolites in 1-year-old mouse tissues

Tissues were harvested from 1-year-old *Bhmt*$^{+/+}$ and *Bhmt*$^{-/-}$ mice. Hepatic AdoMet, AdoHcy, and plasma homocysteine and cysteine were quantified by high pressure liquid chromatography. Choline metabolites were extracted and quantified by liquid chromatography-electrospray ionization-isotope dilution mass spectrometry. Data are presented as mean ± S.E., $n = 8$ per group.

Organ	Metabolites	*Bhmt*$^{+/+}$	*Bhmt*$^{-/-}$
Liver	AdoMet (nmol/g tissue)	113.1 ± 14.7	56.8 ± 3.9[a]
	AdoHcy (nmol/g tissue)	31.9 ± 5.3	176.3 ± 22.1[a]
	AdoMet:AdoHcy	4.05 ± 0.65	0.35 ± 0.03[a]
	Betaine (nmol/g tissue)	1,158 ± 330	34,976 ± 2,700[a]
	Choline (nmol/g tissue)	84 ± 13	144 ± 26
	GPCho (nmol/g tissue)	803 ± 121	218 ± 21[a]
	PC (nmol/g tissue)	674 ± 90	243 ± 59[a]
	PtdCho (nmol/g tissue)	17,317 ± 683	14,075 ± 795[a]
	Sphingomyelin (nmol/g tissue)	1,788 ± 127	1,976 ± 85
Plasma	tHomocysteine (μM)	5.5 ± 0.7	37.7 ± 8.6[a]
	Cysteine (μM)	150.8 ± 17.4	134.6 ± 23.1

[a] $p < 0.01$, different from *Bhmt*$^{+/+}$ by Student's *t* test.

DISCUSSION

To our knowledge, this is the first report of the successful creation of *Bhmt*$^{-/-}$ mice. Deletion of the *Bhmt* gene resulted in the complete loss of BHMT activity in liver, the organ where nearly all of activity resides in mice. Heterozygous mice had 53% of the hepatic BHMT activity measured in *Bhmt*$^{+/+}$, suggesting that the *Bhmt* gene is biallelically expressed. Mating pairs of *Bhmt*$^{+/+}$, *Bhmt*$^{+/-}$, and *Bhmt*$^{-/-}$ produced offspring with a normal number of pups and evenly distributed genders, suggesting that BHMT is not essential for reproduction. This is interesting because mice in which choline dehydrogenase (*Chdh*; form betaine from choline, immediately upstream from *Bhmt* in choline pathway, Fig. 5) was deleted are infertile (30). Fetuses from heterozygous (*Bhmt*$^{+/-}$) mating pairs were born at the expected Mendelian ratio; they were viable and survived to at least 1 year of age, suggesting that BHMT is not essential for embryonic development or for the viability of mice.

Although a *Bhmt* knock-out mouse has not been previously created, when *S*-(α-carboxybutyl)-DL-homocysteine (CBHcy; a potent and specific inhibitor of BHMT) was administered intraperitoneally to wild type mice (31) or fed to rats (32), it caused an elevation of plasma Hcy concentrations and a reduction in the hepatic AdoMet:AdoHcy ratio. Our current study confirms the finding that inhibiting or ablating flux through BHMT affects one carbon metabolism. The changes are summarized in Fig. 5. As expected, *Bhmt*$^{-/-}$ mice had significantly higher con-

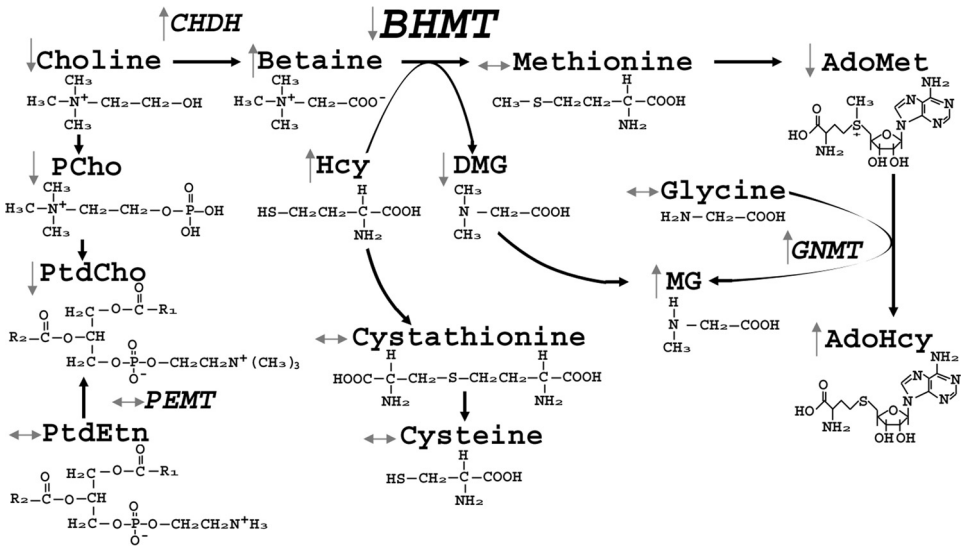

FIGURE 5. **Changes in one-carbon metabolism due to *Bhmt* deletion.** Deletion of *Bhmt* resulted in changes in the concentrations of the metabolites or activities of enzymes involved in homocysteine and one-carbon metabolism in tissues.

centrations of the substrates for this enzyme (betaine and Hcy) in various tissues as compared with $Bhmt^{+/+}$ mice. Our data show that the transsulfuration and methionine synthase pathways do not have the capacity to remove excess tHcy that accumulates when BHMT is not present, indicating that BHMT has a critical role in Hcy homeostasis. $Bhmt^{-/-}$ mice also had a significant reduction in hepatic dimethylglycine concentrations, one of the products of BHMT. Methionine, the other reaction product, was not affected by the gene deletion, probably because dietary methionine and protein stores of methionine are so large that the loss of BHMT-catalyzed biosynthesis does not alter overall concentrations of this amino acid. However, AdoMet concentration, which is formed from methionine, was reduced in livers of $Bhmt^{-/-}$ mice, whereas AdoHcy concentrations were elevated. AdoMet is used by GNMT to form methylglycine from glycine (33) (Fig. 5). Methylglycine is also formed from dimethylglycine, the product of the BHMT catalyzed reaction. Because $Bhmt^{-/-}$ mice do not accumulate dimethylglycine, the elevated methylglycine observed in $Bhmt^{-/-}$ mice likely comes from the action of GNMT. GNMT is allosterically inhibited by methyl-THF (13), which serves as the methyl donor for methionine synthase, a parallel pathway to BHMT that catalyzes the conversion of Hcy to methionine (9). It is possible that the $Bhmt^{-/-}$ mice rely heavily on the use of methyl-THF to form the needed methionine. Hence, GNMT is released from methyl-THF inhibition, resulting in increased methylglycine, reduced AdoMet and increased AdoHcy concentrations that we observed. This hypothesis is supported by elevated hepatic GNMT activity in $Bhmt^{-/-}$ mice (Fig. 2), as well as the reduction in plasma concentrations of total folate (the predominant form contributing to plasma total folate is methyl-THF) (Table 2). AdoHcy is cleaved by AdoHcy hydrolase, producing Hcy and adenosine. This reaction is reversible and thermodynamically favors the synthesis of AdoHcy (34); this should occur in the presence of the high tHcy concentrations present in the $Bhmt^{-/-}$ mice.

Despite high plasma tHcy concentrations, $Bhmt^{-/-}$ mice had significantly lower plasma cysteine concentrations; we observed no differences in hepatic cysteine concentrations. Normally, high Hcy would be expected to result in increased cystathionine and cysteine concentrations. For example, methylenetetrahydrofolate reductase-deficient mice had elevated plasma Hcy, accompanied by elevated plasma cysteine (35). Supplemental betaine has been shown to increase the activity of liver CBS (36), thus the accumulation of this metabolite as well as tHcy in $Bhmt^{-/-}$ mice would be expected to increase concentrations of cysteine. However, AdoMet is an allosteric activator of CBS (37), and we suggest that reduced hepatic AdoMet concentrations inhibit the transsulfuration pathway. The flux of cysteine from liver to plasma must be rapid, perhaps explaining why plasma and not hepatic cysteine concentrations are altered.

Deletion of *Bhmt* results in a substantial accumulation of betaine in most tissues except testis. Betaine is either used as a methyl donor (which is blocked by *Bhmt* deletion) or as an osmolyte that regulates cellular volume and fluid balance. The accumulation of betaine in $Bhmt^{-/-}$ mice may affect osmoregulation. Tests of kidney function did not reveal any malfunction (Table 3). However, $Bhmt^{-/-}$ mice had reduced urinary specific gravity compared with that of $Bhmt^{+/+}$ mice (Table 3), suggesting reduced reabsorption of water by the kidney tubule. This finding is puzzling because high betaine should result in increased reabsorption of water and increased urine osmolality.

Surprisingly, the deletion of *Bhmt* does not result in accumulation of choline, the precursor of betaine. Choline is either oxidized to form betaine by the enzyme CHDH or it is used to form PtdCho. Because $Bhmt^{-/-}$ mice cannot utilize betaine, we expected to see product inhibition of CHDH resulting in increased choline availability for use in PtdCho synthesis. We observed the opposite, with lower choline and PtdCho concentrations in a number of tissues. $Bhmt^{-/-}$ mice had elevated hepatic expression of *Chdh* (data not shown) and hepatic CHDH activity (Fig. 2), suggesting that this gene is induced by some factor in $Bhmt^{-/-}$ mice, possibly explaining increased use of choline to form betaine. The regulatory mechanisms for such an effect are not known.

At 5 weeks of age, *Bhmt*$^{-/-}$ mice developed a fatty liver, and had elevated plasma ALT activity (a measure of hepatic damage). The fatty liver is the result of decreased synthesis of PtdCho, which is essential for the secretion of VLDL from liver (38). These findings are consistent with the literature. Rodents and humans fed a choline-deficient diet develop fatty liver (39, 40), and have elevated plasma ALT activity because choline deficiency induces hepatocytes apoptosis (41). Consistent with these observations in *Bhmt*$^{-/-}$ mice, others have reported administration of betaine or the induction of BHMT activity prevents fatty liver in *Mthfr*$^{-/-}$ mice (35), in nonalcoholic fatty liver (42), and in alcohol-induced fatty livers (43, 44) in rodents. Together, these data suggest the importance of BHMT activity in modulating hepatic steatosis. In addition, *Bhmt*$^{-/-}$ mice had reduced plasma total cholesterol and HDL-C. The role of *Bhmt* deletion in cholesterol and lipoprotein homeostasis warrants further studies.

At 1 year of age, 64% of *Bhmt*$^{-/-}$ mice developed hepatic tumors. Histopathology confirmed that these tumors were either hepatocellular adenomas or carcinomas. Even those that did not have visible tumors had a higher incidence of fat accumulation, cellular alteration, and hyperplasia when compared with *Bhmt*$^{+/+}$ livers. Histological modifications were accompanied by elevation in γGT1 levels, a highly sensitive marker of HCC. In rodents, choline deficiency results in a higher incidence of spontaneous hepatocellular carcinomas (45). Several mechanisms are suggested for these carcinogenic effects. Choline deficiency increases lipid peroxidation in the liver (46), which is a source of free radicals in the nucleus that could modify DNA and cause carcinogenesis. Choline deficiency perturbs protein kinase C signaling, resulting in altered cell proliferation signals and cell apoptosis and eventually in carcinogenesis (40). Methyl deficiency may also mediate the mechanisms that underlie the etiology of cancers. AdoMet levels control cell growth, and a persistent decrease in AdoMet concentrations leads to the development of HCC as observed in the methionine adenosyltranferase 1A knock-out mouse model (cannot make AdoMet from Met) (48). Methyl deficiency may also alter epigenetic machinery by hypomethylating some genes but paradoxically hypermethylating specific genes (tumor suppressor genes) and consequently increasing the recruitment of methyl-binding proteins to the CpG islands. Consequently, the expression of tumor suppressor genes responsible for DNA repair (BRCA1, hMLH1), cell cycle regulation (p15, p16), carcinogenesis metabolism (GSTP1), hormonal response (RARβ2), apoptosis (DAPK, APAF-1), and cell adherence (CDH1, CDH3) (49–51) are silenced, leading to tumor development. All the above mechanisms are potentially the underlying causes of HCC observed in *Bhmt*$^{-/-}$ mice because these mice are essentially choline and methyl-group deficient. We plan to investigate each of these hypotheses in ongoing work in our laboratory.

Hepatocellular carcinoma is the fifth most common type of cancer worldwide (52). In mouse models harboring genetic defects, HCC occurs spontaneously in a very limited number of cases (47). For the first time, we present evidence that *Bhmt* gene dysfunction links a metabolic defect to spontaneous neoplastic transformation in rodent livers. *Bhmt*$^{-/-}$ mice model marks the upper boundary for an effect of a lost-of-function gene variant in humans. Our studies in the *Bhmt*$^{-/-}$ mice suggest that humans with lost-of-function mutation in the *BHMT* gene may have important consequences, including hyperhomocysteinemia, altered choline metabolites, fatty liver, and hepatocellular carcinomas. It would be interesting to explore whether enhanced BHMT activity would reverse these symptoms.

Acknowledgments—We thank Dr. Corneliu Craciunescu, Dr. Randy Thresher, Dr. Virginia Godfrey, Dr. Arlin Rogers, Dr. Sally Stabler, Dr. Lance Johnson, Dr. Zhong Guo, and Friday Walter for analytic assistance.

REFERENCES

1. Feng, Q., Kalari, K., Fridley, B. L., Jenkins, G., Ji, Y., Abo, R., Hebbring, S., Zhang, J., Nye, M. D., Leeder, J. S., and Weinshilboum, R. M. (2011) *Mol. Genet. Metab.* **102,** 126–133
2. da Costa, K. A., Kozyreva, O. G., Song, J., Galanko, J. A., Fischer, L. M., and Zeisel, S. H. (2006) *FASEB J.* **20,** 1336–1344
3. Boyles, A. L., Billups, A. V., Deak, K. L., Siegel, D. G., Mehltretter, L., Slifer, S. H., Bassuk, A. G., Kessler, J. A., Reed, M. C., Nijhout, H. F., George, T. M., Enterline, D. S., Gilbert, J. R., and Speer, M. C. (2006) *Environ. Health Perspect.* **114,** 1547–1552
4. Weisberg, I. S., Park, E., Ballman, K. V., Berger, P., Nunn, M., Suh, D. S., Breksa, A. P., 3rd, Garrow, T. A., and Rozen, R. (2003) *Atherosclerosis* **167,** 205–214
5. Xu, X., Gammon, M. D., Zeisel, S. H., Bradshaw, P. T., Wetmur, J. G., Teitelbaum, S. L., Neugut, A. I., Santella, R. M., and Chen, J. (2009) *FASEB J.* **23,** 4022–4028
6. Szegedi, S. S., Castro, C. C., Koutmos, M., and Garrow, T. A. (2008) *J. Biol. Chem.* **283,** 8939–8945
7. Zeisel, S. H. (2006) *Annu. Rev. Nutr.* **26,** 229–250
8. Pajares, M. A., and Pérez-Sala, D. (2006) *Cell Mol. Life Sci.* **63,** 2792–2803
9. Selhub, J. (1999) *Annu. Rev. Nutr.* **19,** 217–246
10. Delgado-Reyes, C. V., Wallig, M. A., and Garrow, T. A. (2001) *Arch. Biochem. Biophys.* **393,** 184–186
11. Garrow, T. A. (1996) *J. Biol. Chem.* **271,** 22831–22838
12. Grossman, E. B., and Herbert, S. C. (1989) *Am. J. Physiol.* **256,** F107–F112
13. Wagner, C., Briggs, W. T., and Cook, R. J. (1985) *Biochem. Biophys. Res. Commun.* **127,** 746–752
14. Ridgway, N. D., and Vance, D. E. (1988) *J. Biol. Chem.* **263,** 16864–16871
15. Ridgway, N. D., and Vance, D. E. (1988) *J. Biol. Chem.* **263,** 16856–16863
16. Bradford, M. M. (1976) *Anal. Biochem.* **72,** 248–254
17. Koc, H., Mar, M. H., Ranasinghe, A., Swenberg, J. A., and Zeisel, S. H. (2002) *Anal. Chem.* **74,** 4734–4740
18. Shivapurkar, N., and Poirier, L. A. (1983) *Carcinogenesis* **4,** 1051–1057
19. Molloy, A. M., Weir, D. G., Kennedy, G., Kennedy, S., and Scott, J. M. (1990) *Biomed. Chromatogr.* **4,** 257–260
20. Ubbink, J. B., Hayward Vermaak, W. J., and Bissbort, S. (1991) *J. Chromatogr.* **565,** 441–446
21. Stabler, S. P., Sekhar, J., Allen, R. H., O'Neill, H. C., and White, C. W. (2009) *Free Radic. Biol. Med.* **47,** 1147–1153
22. Horne, D. W., and Patterson, D. (1988) *Clin. Chem.* **34,** 2357–2359
23. Bligh, E. G., and Dyer, W. J. (1959) *Can. J. Biochem. Physiol.* **37,** 911–917
24. Watkins, S. M., Lin, T. Y., Davis, R. M., Ching, J. R., DePeters, E. J., Halpern, G. M., Walzem, R. L., and German, J. B. (2001) *Lipids* **36,** 247–254
25. Svanborg, A., and Svennerholm, L. (1961) *Acta Med. Scand.* **169,** 43–49
26. Folch, J., Lees, M., and Sloane Stanley, G. H. (1957) *J. Biol. Chem.* **226,** 497–509
27. Lillie, R. (1965) *Histopathologic Technic and Practical Histochemistry,* 3rd Ed., McGraw-Hill Book Co., New York
28. Lowry, O. H., Rosebrough, N. J., Farr, A. L., and Randall, R. J. (1951) *J. Biol. Chem.* **193,** 265–275
29. Zhou, L., Liu, J., and Luo, F. (2006) *World J. Gastroenterol.* **12,** 1175–1181

30. Johnson, A. R., Craciunescu, C. N., Guo, Z., Teng, Y. W., Thresher, R. J., Blusztajn, J. K., and Zeisel, S. H. (2010) *FASEB J.* **24,** 2752–2761
31. Collinsova, M., Strakova, J., Jiracek, J., and Garrow, T. A. (2006) *J. Nutr.* **136,** 1493–1497
32. Strakova, J., Williams, K. T., Gupta, S., Schalinske, K. L., Kruger, W. D., Rozen, R., Jiracek, J., Li, L., and Garrow, T. A. (2010) *Nutr. Res.* **30,** 492–500
33. Blumenstein, J., and Williams, G. R. (1963) *Can. J. Biochem. Physiol.* **41,** 201–210
34. Finkelstein, J. D. (1990) *J. Nutr. Biochem.* **1,** 228–237
35. Schwahn, B. C., Chen, Z., Laryea, M. D., Wendel, U., Lussier-Cacan, S., Genest, J., Jr., Mar, M. H., Zeisel, S. H., Castro, C., Garrow, T., and Rozen, R. (2003) *FASEB J.* **17,** 512–514
36. Kim, S. K., Choi, K. H., and Kim, Y. C. (2003) *Biochem. Pharmacol.* **65,** 1565–1574
37. Prudova, A., Bauman, Z., Braun, A., Vitvitsky, V., Lu, S. C., and Banerjee, R. (2006) *Proc. Natl. Acad. Sci. U.S.A.* **103,** 6489–6494
38. Noga, A. A., Zhao, Y., and Vance, D. E. (2002) *J. Biol. Chem.* **277,** 42358–42365
39. Fischer, L. M., daCosta, K. A., Kwock, L., Stewart, P. W., Lu, T. S., Stabler, S. P., Allen, R. H., and Zeisel, S. H. (2007) *Am. J. Clin. Nutr.* **85,** 1275–1285
40. da Costa, K. A., Cochary, E. F., Blusztajn, J. K., Garner, S. C., and Zeisel, S. H. (1993) *J. Biol. Chem.* **268,** 2100–2105
41. da Costa, K. A., Badea, M., Fischer, L. M., and Zeisel, S. H. (2004) *Am. J. Clin. Nutr.* **80,** 163–170
42. Kwon do, Y., Jung, Y. S., Kim, S. J., Park, H. K., Park, J. H., and Kim, Y. C. (2009) *J. Nutr.* **139,** 63–68
43. Barak, A. J., Beckenhauer, H. C., Junnila, M., and Tuma, D. J. (1993) *Alcohol Clin. Exp. Res.* **17,** 552–555
44. Kharbanda, K. K., Mailliard, M. E., Baldwin, C. R., Beckenhauer, H. C., Sorrell, M. F., and Tuma, D. J. (2007) *J. Hepatol.* **46,** 314–321
45. Newberne, P. M., and Rogers, A. E. (1986) *Annu. Rev. Nutr.* **6,** 407–432
46. Rushmore, T. H., Lim, Y. P., Farber, E., and Ghoshal, A. K. (1984) *Cancer Lett.* **24,** 251–255
47. Newell, P., Villanueva, A., Friedman, S. L., Koike, K., and Llovet, J. M. (2008) *J. Hepatol.* **48,** 858–879
48. Lu, S. C., and Mato, J. M. (2008) *J. Gastroenterol. Hepatol.* **23,** Suppl. 1, S73–77
49. Costello, J. F., and Plass, C. (2001) *J. Med. Genet.* **38,** 285–303
50. Esteller, M. (2002) *Oncogene* **21,** 5427–5440
51. Momparler, R. L. (2003) *Oncogene* **22,** 6479–6483
52. Feo, F., De Miglio, M. R., Simile, M. M., Muroni, M. R., Calvisi, D. F., Frau, M., and Pascale, R. M. (2006) *Biochim. Biophys. Acta* **1765,** 126–147